MethodsX 13 (2024) 102951

Contents lists available at ScienceDirect

MethodsX

journal homepage: www.elsevier.com/locate/methodsx

Adsorption performance with field emission scanning electron microscopy of fruit peel induced Silver Nanoparticles in $C_{16}H_{18}ClN_3S$ for waste water treatment ☆,☆☆

Jyolsna P, Gowthami V*, Hajeera Aseen A

School of Basic Science, Vels Institute of Science Technology and Advanced Studies, Pallavaram, Chennai, India, 600117

A R T I C L E I N F O

Method name:
Adsorption of pollutants by synthesized nanoparticles

Keywords:
Nanoparticles
Nanoadsorbent
GC–MS
Wastewater Purification

A B S T R A C T

There is a growing demand for cost-effective and sustainable technologies for treating wastewater as water consumption increases and conventional technologies become more expensive. Nanoparticles have a great deal of potential for use in the treatment of waste water. Their unique surface area allows them to effectively remove toxic metal ions, pathogenic microorganisms, organic and inorganic solutes from water. This study investigated the potential of orange and banana peels as renewable nano adsorbents for removing dyes and dissolved organic compounds from textile wastewater. Orange and banana peels are an optimal selection due to their favourable chemical characteristics, namely the presence of cellulose, pectic, hemicellulose, and lignin. Their capacity to adsorb diverse anionic and cationic compounds on their surface-active sites is attributed to their unique functional group compositions. Silver nanoparticles are able to adsorb heavy metals due to their exceptionally low electrical and thermal resistance and surface plasmon resonance. The samples were thoroughly characterised using field emission scanning electron microscopy (FE-SEM), UV–Visible spectrometry, Fourier transform infrared spectroscopy (FTIR) and XRD. The nanoparticles were prepared (10 gm,50 gm,100 gm) and subsequently introduced to the wastewater sample. The optical density values were recorded at various time points. The optical density values demonstrate a decline over the course of the experiment, with a notable decrease observed over time. The results of this study provide valuable insights into the efficacy of these natural adsorbents and their potential for sustainable water purification technologies. For the purpose of this research, high performance instrumentation methods were performed as follows:

- Field emission scanning electron microscopy for surface morphology studies.
- Gas chromatography-mass spectrometry (GC–MS) for analytical technique that combines gas chromatography (GC) and mass spectrometry (MS) to identify unknown substances or contaminants.
- Optical density values were measured for different timings of degradation.

☆ **Related research article:** None.
☆☆ **For a published article:** *NONE.*

* Corresponding author.
E-mail address: gowthami.sbs@velsuniv.ac.in (G. V).

https://doi.org/10.1016/j.mex.2024.102951
Received 5 July 2024; Accepted 6 September 2024
Available online 7 September 2024

Specifications table

Subject area:	Environmental Science
More specific subject area:	Wastewater treatment
Name of your method:	Adsorption of Pollutants by Synthesized Nanoparticles
Name and reference of original method:	*NIL*
Resource availability:	Fruit peels from Koyembedu market, Chennai, Tamilnadu, India

Background

The availability of clean water is of paramount importance for all living organisms, yet it is estimated that almost 800 million individuals globally lack access to suitable water for domestic use .The steady growth in global population, coupled with the expansion of industrial activity and the introduction of new pollutants into the environment, has resulted in the addition of new pollutants to soil, plants, and the wider environment. This is primarily occurring via water pollution, which is giving rise to concerns about the potential risks these pollutants may pose to human health [1,2]. A plethora of contemporary and ongoing water treatment solutions are currently in use, including photocatalytic water purification, desalination, filtration and disinfection. It is imperative that the water supplied to users meets the requisite chemical, biological and physical quality standards at the point of entry into the distribution system [3]. Consequently, the concept of safe drinking water is relative and contingent upon the standards and guidelines established by a given country. The existing body of knowledge on the treatment of purified water remains incomplete in several areas, particularly in regard to the discrepancy between laboratory and field performance of point-of-use water treatment techniques. This shortcoming has been highlighted by [4,5], who have drawn attention to the need for further research in this domain. Furthermore, there is a lack of a comprehensive literature on the monitoring of textile effluents and usage of fruit peels for water purification, which represents another area where further investigation is warranted.

Our idea is to develop an appropriate experimental technique for the evaluation of effluent adsorption in textile wastewater, with the ultimate goal of achieving purification. To achieve this, the theory of adsorption was employed in the study of effluent adsorption by fruit peel-induced metal nanoparticles. The process of adsorption is an exothermic phenomenon that occurs at the surface of a substance. During this phenomenon, a phase of matter, referred to as the adsorbate, transfers from a liquid or gaseous state to a solid or semi-solid state, and subsequently adsorbs on a solid surface, which may or may not be in the liquid state. The transfer occurs via physicochemical or chemical interactions under specific, defined conditions, forming a monomolecular layer on the surface. The choice for an effective reducing agent for metal nanoparticles orange and banana peel extracts due to their rich polyphenol content, which facilitates the synthesis of silver nanoparticles under milder conditions. Additionally, the banana peel extract demonstrated the ability to rapidly reduce silver ions into nanoparticles. This study has the potential to enhance the ease of the purification method compared to existing sophisticated techniques. The proposed research approach is intended to address the shortcomings of conventional laboratory methods by offering a cost-effective, ecologically sound, reproducible, and verifiable analytical technique.

Method details

Collection of fruit peels

Banana and orange peels were sourced from a local supermarket in Koyambedu, Chennai, India. For dye degradation experiments, silver nitrate (99.8 % purity, Kishida) and methylene blue (MB) solution were employed. All experimental solutions were prepared using double distilled water. The fruit peels were collected from the aforementioned supermarket and then processed for further analysis. Subsequently, the peels were cut into small pieces and washed with tap water for approximately five to ten minutes. Following this, a second wash with distilled water was conducted for approximately twenty minutes, the purpose of which was to remove any remaining impurities. Once this was completed, the peels were dried for a period of 24 h at a temperature of 100 °C. Following this drying stage, the peels were ground into a powder, which was then sieved through a 1.40 mm sieve. In order to prepare an extract from both peels, 10 g of combined peel powder was mixed with 200 mL of distilled water. The mixture was then shaken at 150 rpm for one hour and left to incubate overnight at room temperature. The resulting solution was filtered through Whatman No. 4 filter and stored in a conical flask for use in nanoparticle synthesis.

Synthesis of silver nanoparticles (AgNPs) using combined peel extract

The combined peel extract was prepared at room temperature by mixing 20 mL with 80 mL of 1 mM $AgNO_3$ aqueous solution (0.013 g). This solution was then stirred on a magnetic stirrer of 200 rpm for one hour. Following incubation of the final solution ($AgNO_3$ - CPE) in the dark for 24 h at room temperature, a brown color change indicated the formation of nanoparticles. The observed synthesis may be attributed to the presence of reducing agents, which may include polysaccharides, phenolic compounds, alkaloids, or triterpenoids. The initial color shift that occurs during the green synthesis of nanoparticles is predominantly attributable to the surface Plasmon Resonance (SPR) phenomenon. Surface plasmon resonance (SPR) arises from the collective oscillation of free electrons in nanoparticles, which interact with the electromagnetic field of light [6,7]. As a consequence of this interaction, specific wavelengths of light are absorbed, which results in a change in the color of the solution. The specific chromatic alteration observed is dependent

on the type of nanoparticle undergoing synthesis. For example, the color change exhibited by silver nanoparticles typically progresses from pale yellow to brown, whereas gold nanoparticles display a color change from pale red to deep red [8,9]. This color change serves as a visual indication of the successful formation of nanoparticles. Additionally, other factors may contribute to the initial color change, including the presence of plant extract components, such as flavonoids and phenolics, which have the capacity to absorb light, thereby influencing the observed change in color. In summary, the initial color change observed during green synthesis of nanoparticles provides an invaluable indicator of the successful formation of nanoparticles, offering a simple and non-invasive method for monitoring the synthesis process Furthermore, the formation of silver nanoparticles was corroborated by the appearance of a strong surface plasmon resonance (SPR) band in the ultraviolet-visible (UV–Vis) spectrum, peaking at approximately 400–450 nm [10–12].

Preparation of methylene blue solution

To prepare a solution containing 2.5 ppm of methylene blue, the requisite quantity of methylene blue solution was mixed with distilled water. For a 500-ml solution, 0.1 g of methylene blue solution was used. The dye solution was subsequently placed in a shaker for one hour to ensure uniform dispersion. After one hour, the solution was divided into three100-ml flasks and silver nanoparticles was added. The flasks were placed in a shaker for one hour, and a comparative study was conducted by drying repeating the same procedure.

Characterization techniques

The spectra of the solution were obtained utilizing a UV-5800 PC spectrophotometer and quartz cuvettes in the wavelength range λ= 190–700 nm. A gas chromatography-mass spectrometry (GC–MS) analysis was conducted on a GC 7890 (Agilent) instrument, comprising an automated liquid sampler and a gas chromatograph connected to a mass spectrometer (GC–MS). The carrier gas was helium, with the injector temperature maintained at 350 ˚C. The oven temperature was programmed from 100 ˚C to 375 ˚C at 200 ˚C/min. The name, molecular weight and structural formula of the component were determined. The dimensions of the nanoparticles and the adsorption of methylene blue on the surface of the nanoparticles were determined by field emission scanning electron microscopy (FESEM). Additionally, Fourier transform infrared spectroscopy (FTIR) spectra were generated for both peel and synthetic nanoparticles using a Thermo-Scientific (Bruker Vertex 80) FT-IR spectrophotometer.

Method validation

Analysis of FESEM

The surface morphology of synthetic combined peel containing silver nanoparticles was analyzed using field emission scanning electron microscopy (FESEM). The nanoparticles are spherical and dispersed in a uniform manner. The produced nanoparticles had an average size of 38.2 nm. Fig. 2.a shows agglomerates of small grains and some dispersed particles. Fig. 2.b represents the spherical shape of all nanoparticle present and size was calculated by “Image J software” with varying degree of agglomeration. The FESEM analysis unambiguously demonstrates that the physical microstructure of the combine peel extract-$AgNO_3$ and Ag nanoparticles differs significantly. The small size and good distribution of particles present on the CPE-$AgNO_3$ surface result in a significantly increased effective surface area, thereby increasing the adsorbent’s surface area available for interactions. As demonstrated in the FESEM micrograph Fig. 1.a, the particles exhibited a diverse range of granular sizes, including coarse and fine particles. The formation of spherical nanoparticles enables the encapsulation of active ingredients within a protective polymer matrix, preventing degradation caused by chemical and enzymatic processes. The spherical nanoparticles facilitate the formation of hydrophobic interactions, hydrogen bonds, and electrostatic interactions, leading to the development of robust chemical bonds, such as covalent bonds, between the surface and adsorbed molecules during adsorption. This finding is in contrast to the commercial standard AgNPs, which typically exhibit a diameter of 10–20 nm [13,14]. The study by the group of researchers demonstrated the successful synthesis of various single-crystalline silver nanostructures, such as dendrites, dendritic flowers, and cactus-like rods, through a simple, facile, and cost-effective method [14–16].

UV–Visible spectrum analysis

The ultraviolet–visible (UV–Vis) absorbance maxima for the nanoparticles were identified in the range from approximately 370 to 430 nm, with a visible shift of 443 nm being observed for the current nanoparticles (Fig. 3). The location of the maximum depends on the size and effective shape of the nanostructures. UV–Vis spectra of nanoparticles synthesized in the presence of plant extracts and the spectra of the plant extracts themselves reveal an increase in the intensity of the recorded bands (hyperchromic effect) in the presence of Ag. Metal nanoparticles have free electrons that give rise to a surface plasmon resonance (SPR) absorption band because the electrons of the metal nanoparticles vibrate with each other and resonate with light waves. The surface plasmon resonance characteristics of silver nanoparticles are shown by the appearance of the peaks. In accordance with the available literature on the subject, absorption bands for pure silver are expected to be observed above 390 nm [17–19]. The signal registration below a wavelength of 390 nm indicates the presence of impurities, organic compounds, or solvent residues in the sample [20,21]. The shift of the peak towards higher wavelengths is indicative of the growth of nanoparticles. The registration of such a signal implies

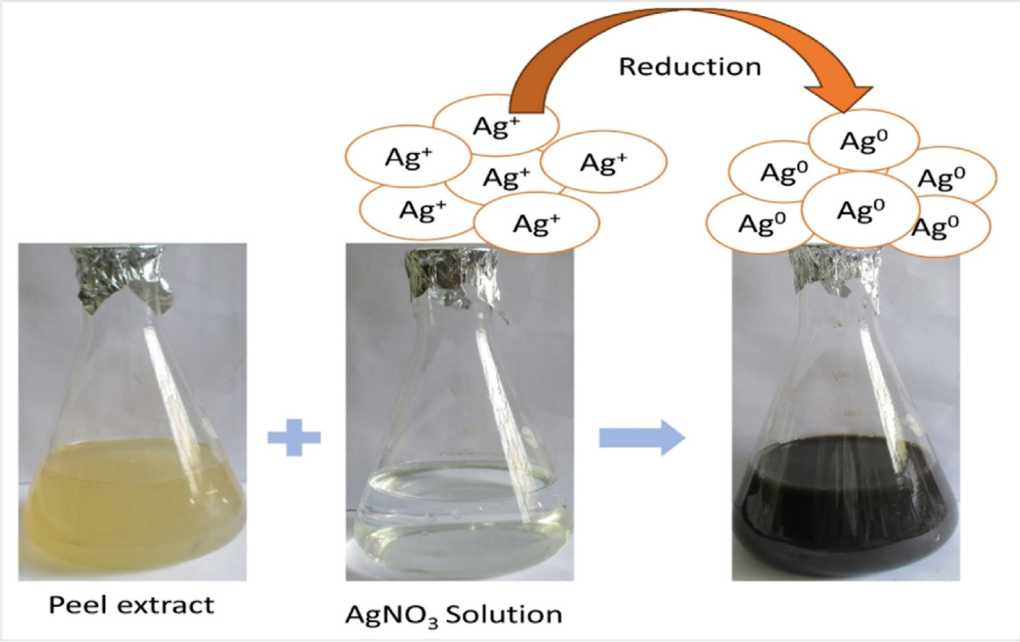

Fig. 1. Synthesis of combined fruit peel and $AgNO_3$ to nanoparticles.

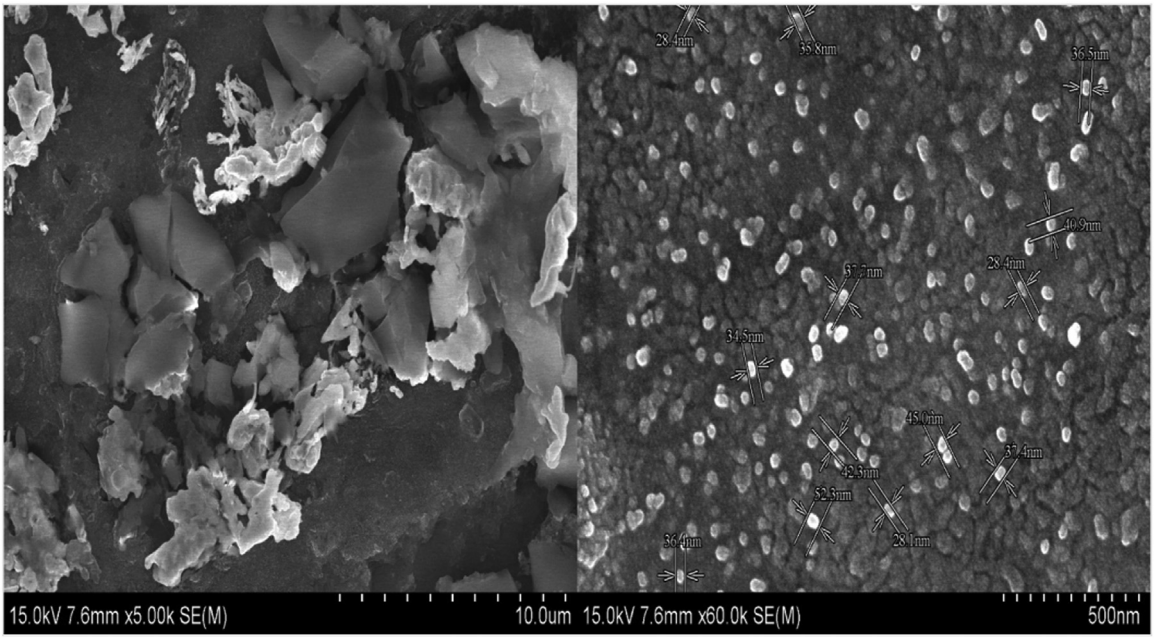

Fig. 2. FESEM images of a) Peel extract and $AgNO_3$ b) CPE-AgNPs with average size of 38.2 nm.

the presence of well-dispersed particles that do not aggregate. According to this literature [22], spherical silver nanoparticles with a diameter less than 100 nm exhibit plasmon resonance in the ultraviolet-visible spectra between 400 and 470–500 nm, with the exact wavelength dependent on their size. This observation is in accordance with the findings of [23,24].

FTIR analysis

FT-IR spectroscopy was employed to identify the predominant functional groups present in the surface structure of CPE-Ag nanoparticles and their potential involvement in the synthesis and stabilization of silver nanoparticles. The resulting spectra of

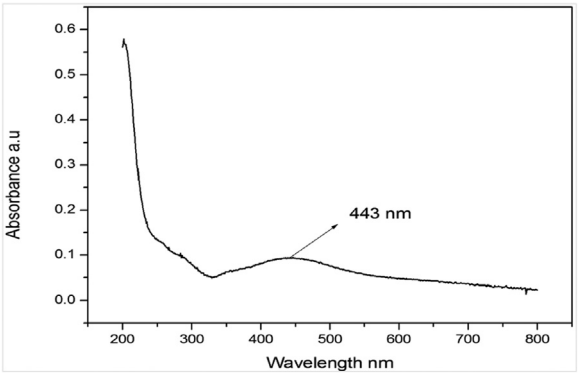

Fig. 3. UV–Visible spectra of CPE-AgNPs.

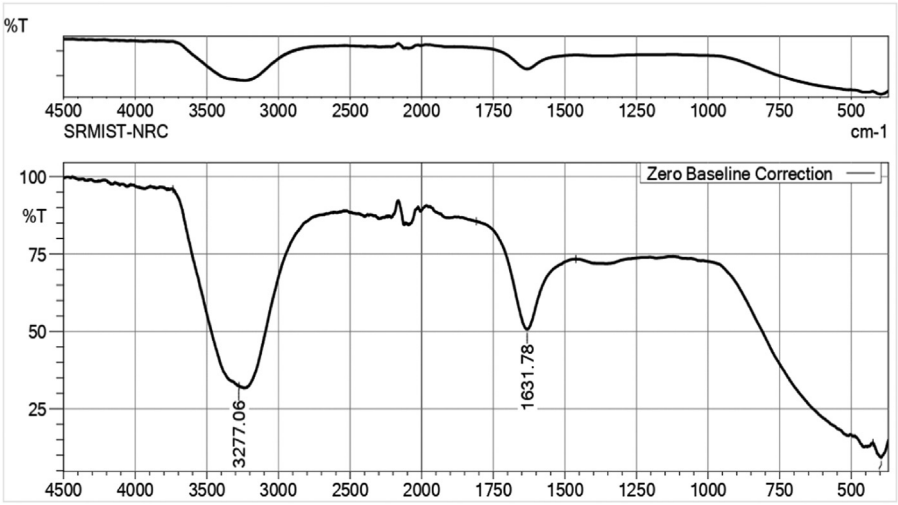

Fig. 4. FTIR spectra of CPE-AgNPs.

CPE-Ag nanoparticles are displayed in the accompanying Fig. 4. The observed bands were found at wavenumbers 1631.78 cm^{-1} and 3277.06 cm^{-1}. The infrared spectrum was assigned to a number of functional groups. These included O–H stretching vibrations associated with alcohols and carboxylic acids, C–O carboxylic acid or alcohol ester, N–C=O amide I bond of proteins, CH_2 alkanes, C–O carboxylic acid, ester or ether, C–N aliphatic amines or alcohol/phenol, N–H distortion of amines, and C–C bending. Subsequent to the reaction with AgNO3, there was observed a shift in the peaks, as indicated in the following spectral analysis: the absorption bands exhibited a range from 3411 to 3281.34 cm^{-1}, indicative of the involvement of carboxyl, hydroxyl, and amide groups, along with the characteristic stretching C=O of COOH at 1631.78 cm^{-1}, which were present on the surface of CPE-Ag nanoparticles synthesis. It can be postulated that the immediate reduction and capping of silver ion into silver nanoparticle observed in the present analysis may be due to the presence of flavonoids and proteins. The flavonoids present in the peel extract have been shown to be powerful reducing agents, and thus may play a role in the formation of AgNPs through the reduction of silver nitrate. Similarly, the flavonoid compounds present in the water extract of peel could be involved in and responsible for the reduction of Ag^+ to Ag^0. These polymers and protein matter can facilitate the reduction of Ag^+ to Ag^0 due to their functional groups. Metal salts are known to interact with biological components through functional groups that mediate the reduction of these salts to nanoparticles [25–27].

GCMS analysis

Gas chromatography and mass spectrometry analysis has been done for both orange peel and banana peel (Figs 5 and 6) The highest peak indicated the presence of eight compounds in the extract, as follows: Vitamin E (31.3 %), 1,2 benzenedicarboxylic acid mono (2-ethylhexylester) (13.47 %), β-tocopherol (11.37 %) and estragole (11.18 %). Compound 1 was identified as anestragole and was found to have a molecular formula of $C_{10}H_{12}O$ (*M/Z* 148) with a retention time of 5.8 min .It has been reported in the literature that this compound has many biological effects, including antioxidant and antimicrobial activities and have studied the effects of this compound on skeletal muscle [34]. The second compound, identified as hexadecanoic acid ethylester, has the molecular formula (*M/Z* 284)). This ester can act as an antioxidant, a hypocholesterolemic agent, a nematicide, a pesticide, a lubricant, and a

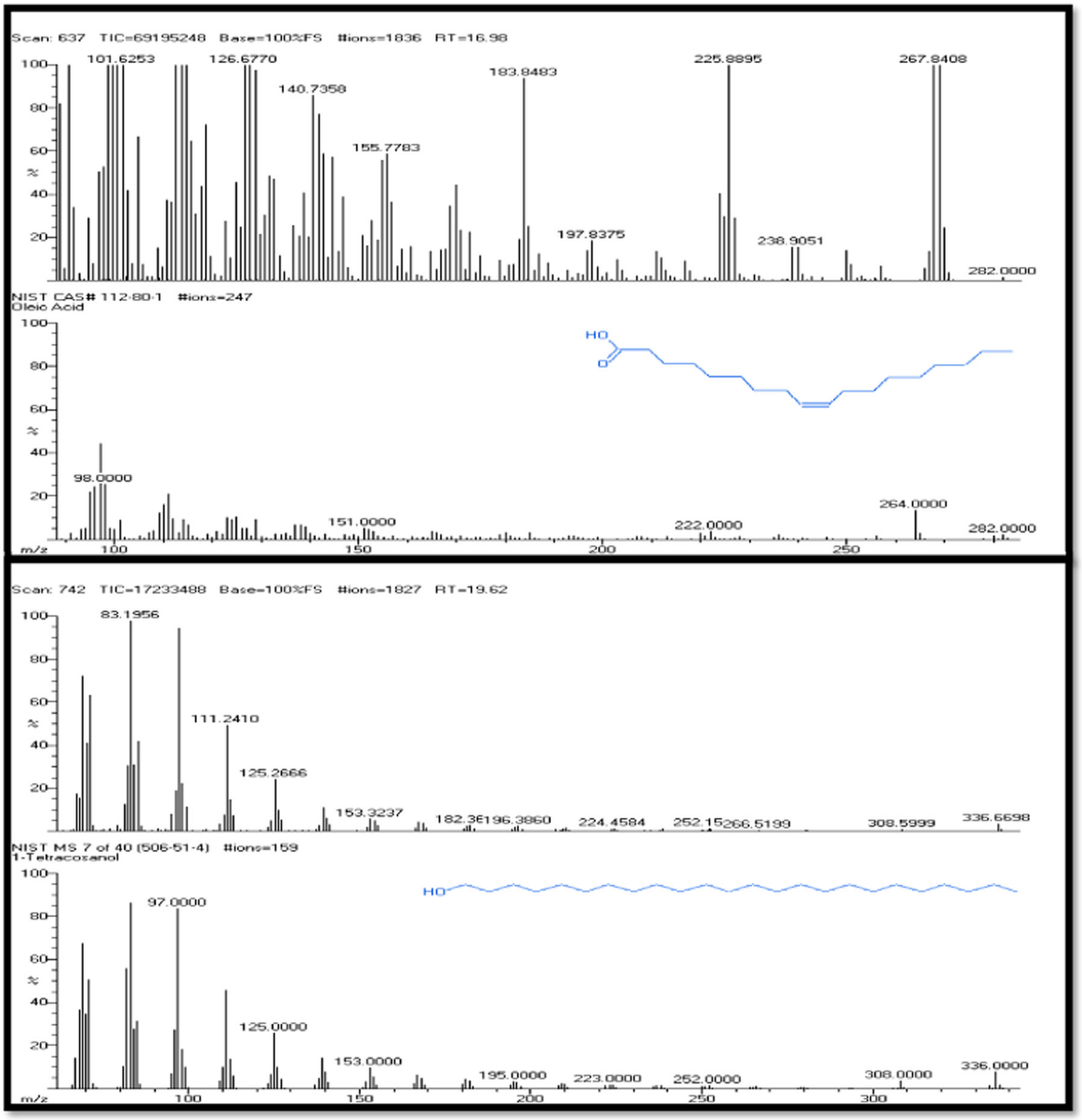

Fig. 5. GCMS of Citrus X Sinensis (Orange peel).

haemolytic inhibitor. Additionally, it functions as a reductase inhibitor. Further analysis revealed that the compound 3 was in fact epicatechin, with a molecular formula of $C_{15}H_{14}O_6$, with a mass-to-charge ratio of 290. Catechin and epicatechin represent two of the most prevalent catechins in dietary sources, with documented benefits for human health. In recent years, they have been employed as antioxidants in lipid oxidation, particularly in oils and fats. Furthermore, they are utilized as an active ingredient in a range of functional foods and dietary supplements. In a recent study, [35] investigated the protective effects of epicatechin against the toxic effects of streptozotocin on rat pancreatic islets. Their findings suggest that epicatechin may offer protection to pancreatic islets against the effects of exposure to streptozotocin, both in vitro and in vivo. The compound 4, identified as gallocatechin, has a molecular formula of $C_{15}H_{14}O_7$ (M/Z −306). Gallocatechin has been demonstrated to possess antimetastatic effects and antidiabetic activity, as well as acting as an antiskin cancer agent. Gallocatechin – epigallocatechin has been shown to exhibit the most potent inhibitory activity on alpha-glucosidase. Gallocatechin has been found to possess anti-uveal melanoma activity, antioxidant and anti-inflammatory properties. In the present study, a GC–MS chromatogram of the orange peel oil extract of Citrus sinensis displayed 15 peaks, indicating the presence of 15 compounds. GC–MS analysis revealed the presence of 15 distinct compounds. The major compounds identified included 5,5,10,10-Tetrachlorotricyclo[7.1.0.0(4,6)] decane, butane, and 1-(2,2-dichloro-3,3-dimethylcyclopropyl) The identified chemical compounds included pentane, 3-chloro-2-nitrobenzyl alcohol,

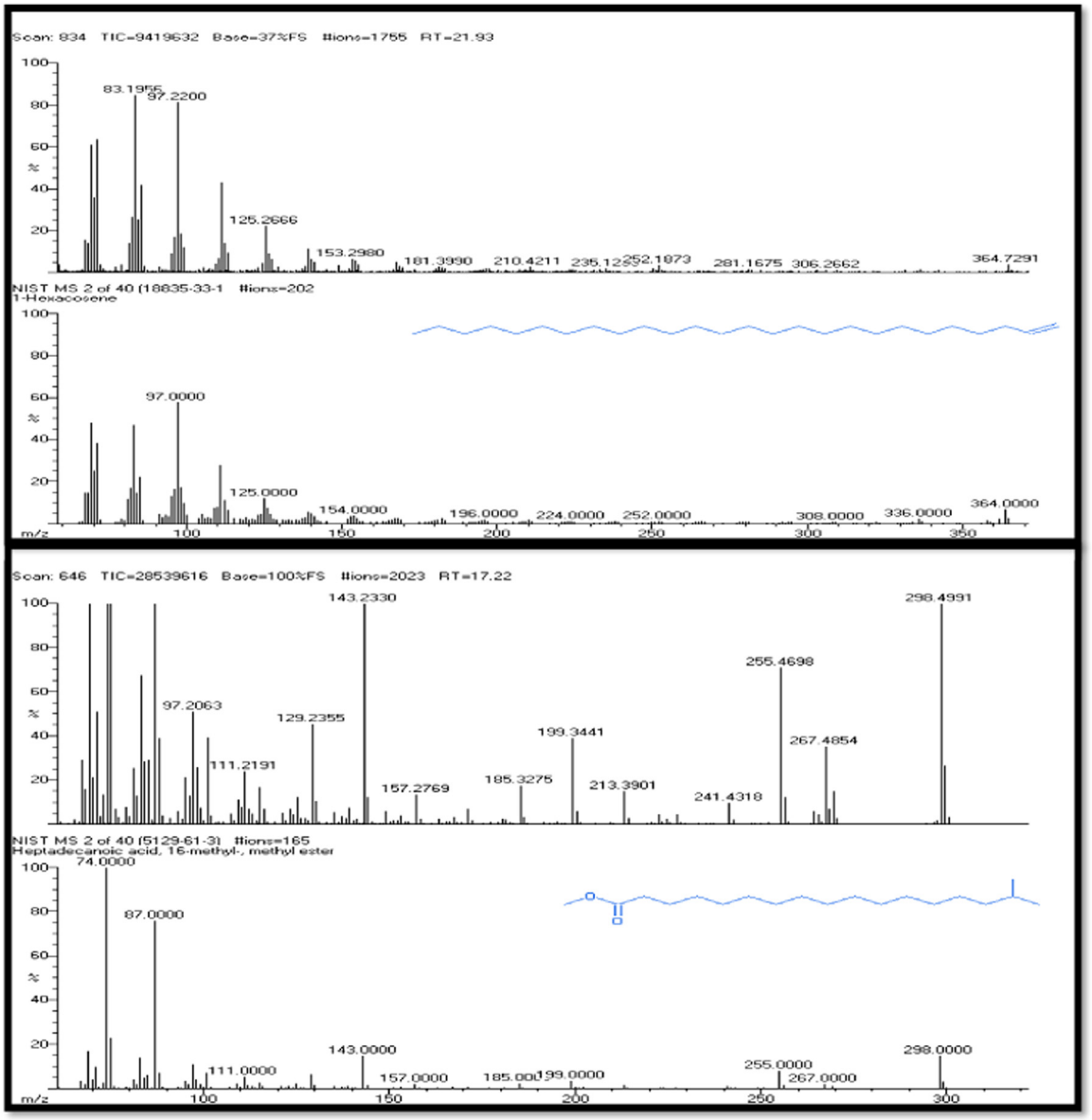

Fig. 6. GCMS of Musa Cavendish (Banana peel).

1-oxaspiro[2.5]octan-4-one, d-limonene, cyclohexanol, beta.-terpinyl acetate, gamma.-terpinene, and 4-terpinenyl acetate. The gas chromatography–mass spectrometry (GC–MS) analyses revealed that the orange peel oil extract is predominantly composed of terpene hydrocarbons and oxygenated compounds, with a small proportion of non-volatile compounds. Terpene fractions typically account for between 50 % and over 95 % of the oil. Citrus species peels are known to contain over 70 % limonene [28,29].

Methylene blue ($C_{16}H_{18}ClN_3S$) degradation using combined peel extract with different timings

The catalytic degradation ability of green produced silver nanoparticles was investigated by preparing a certain concentration of methylene blue solution (Table 1). The produced solution with 0.1 g of methylene blue as control was then mixed with green manufactured nanoparticles and the degradation was monitored at various doses. The degradation of methylene blue into a colorless form could be spectrophotometrically tracked at maximum absorption at 438 nm (Fig. 7). Maximum adsorption was at observed at 7 h of mixing. Additionally, the degradation of methylene blue was observed when combined peel was used. This could be used for comparison investigations. The observed degradation of methylene blue in the absence of nanoparticles was found to be less pronounced than that observed in the presence of nanoparticles, indicating that the addition of nanoparticles improves the degradation efficiency. The absorption value corresponding to the MB n→π^* transition represents the highest absorption peak for pure MB. The

Table 1
OD values for different concentration at different timings.

Concentration (mg)/OD	9.00AM	11.00AM	1.00PM	3.00PM	5.00PM	8.00PM
10	0.92	0.92	0.88	0.88	0.86	0.82
50	0.78	0.65	0.53	0.50	0.47	0.37
100	0.69	0.44	0.38	0.35	0.33	0.27

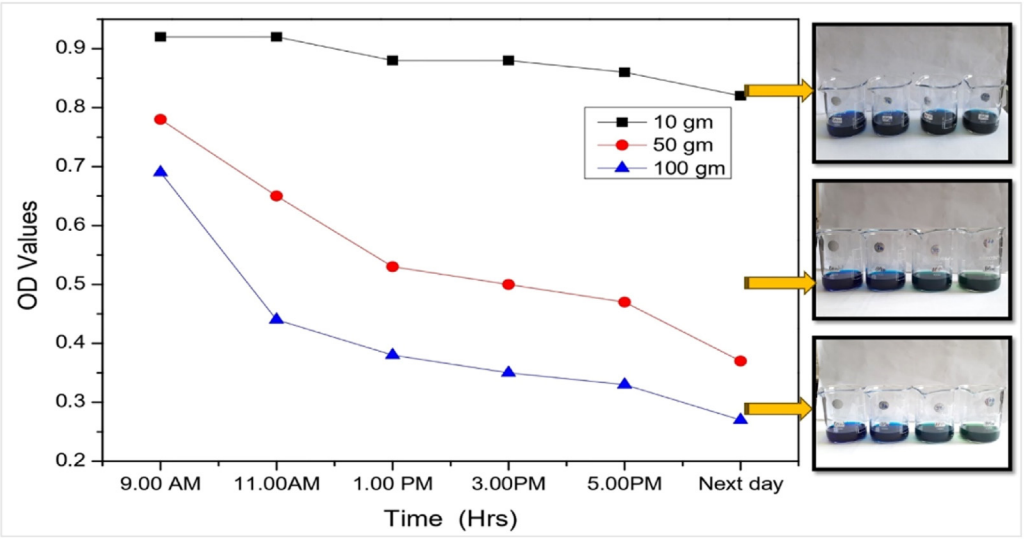

Fig. 7. Degradation graph at different timings and visual observations.

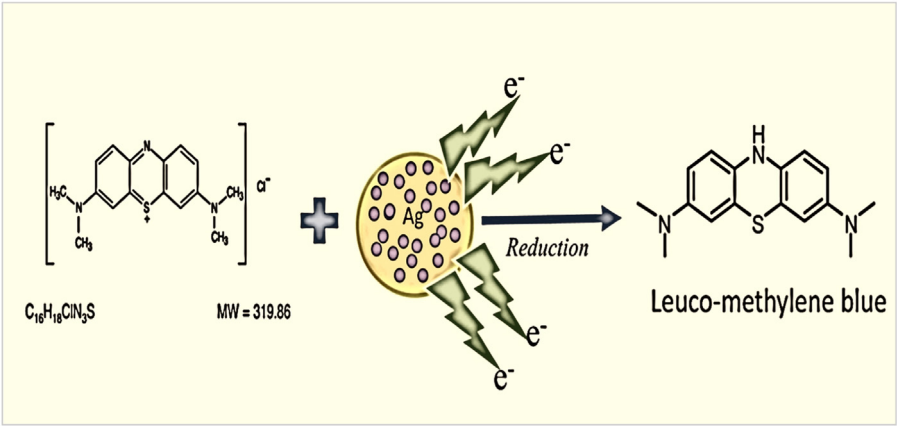

Fig. 8. Possible adsorption mechanism by AgNPs.

larger surface area of silver nanoparticles (NPs) and their composites compared to other NPs leads to enhanced catalytic activity in the removal and degradation of dyes (Fig. 8. [30,31] investigated the reduction of MB by biosynthesized AgNPs and during the process, slow reduction was observed in the presence of the powerful reducing agent $NaBH_4$. The absorption of biosynthesized AgNPs with a rate constant of 0.056 min^{-1} is interpreted by our results. The outcomes were consistent with those observed in previous studies investigating the efficiency of biosynthesized AgNPs in catalytic and adsorption kinetic investigations of MB dye. The breakdown of colors is commonly achieved through the use of $NaBH_4$, a powerful reducing agent.

FESEM analysis after adsorption

Figs. 9–11 depicts the removal efficiency and adsorption capacity at varying dosages of adsorbent materials. The adsorption removal efficiency is seen to increase with an increased adsorbent dose due to the expansion of the available surface area and an increase in the number of adsorption active sites. Conversely, the capacity of adsorption decreases with the increase in dosage. The

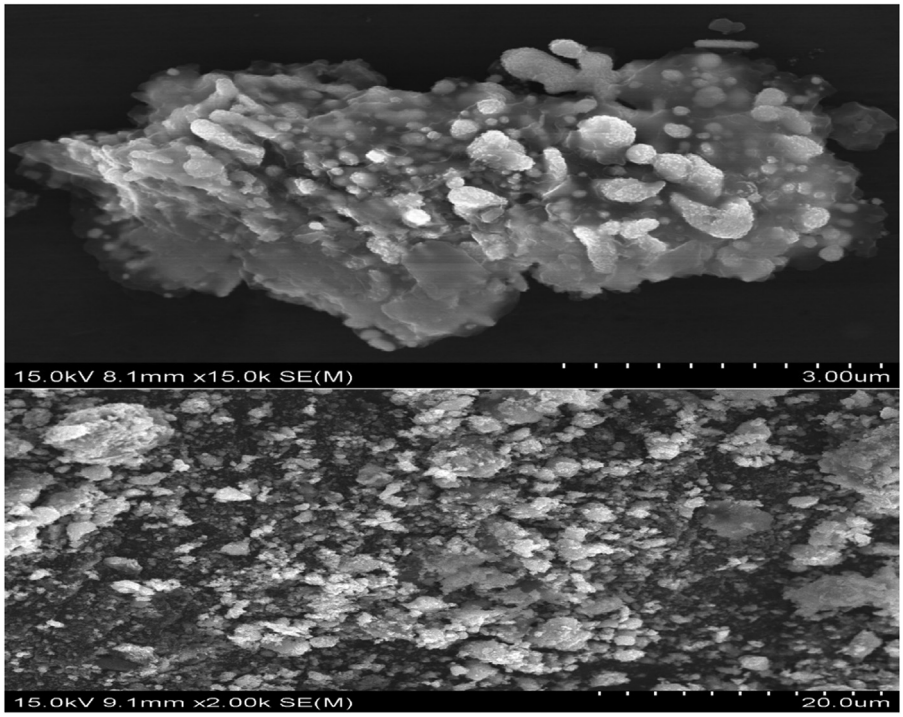

Fig. 9. FESEM images of adsorption of $C_{16}H_{18}ClN_3S$ for 10 gm.

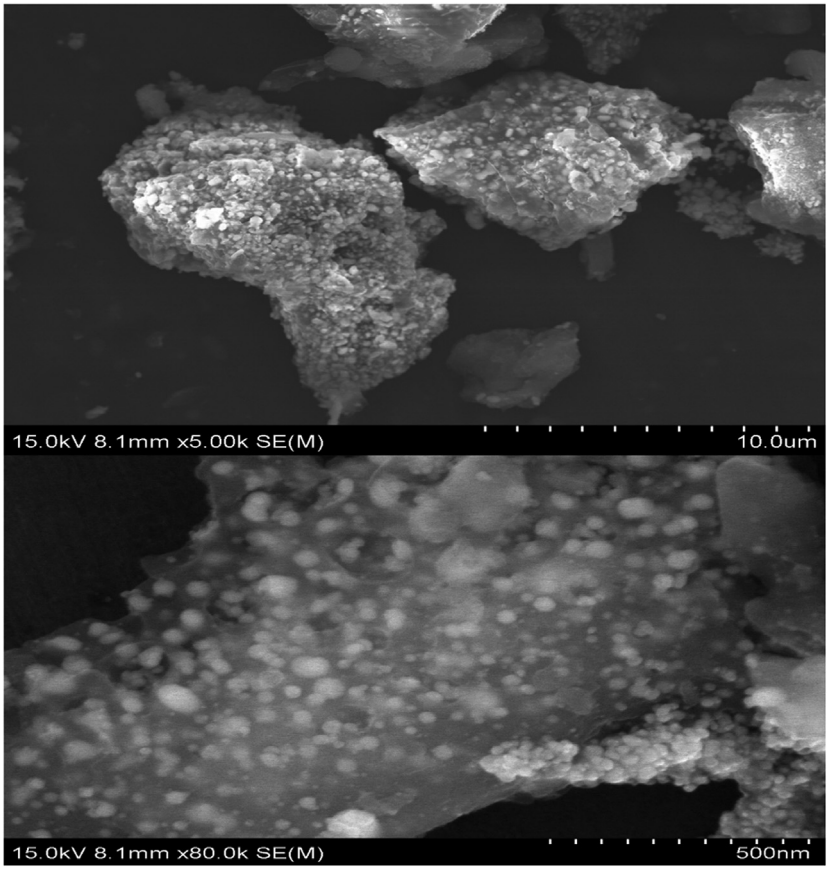

Fig. 10. FESEM images of adsorption of $C_{16}H_{18}ClN_3S$ for 50 gm.

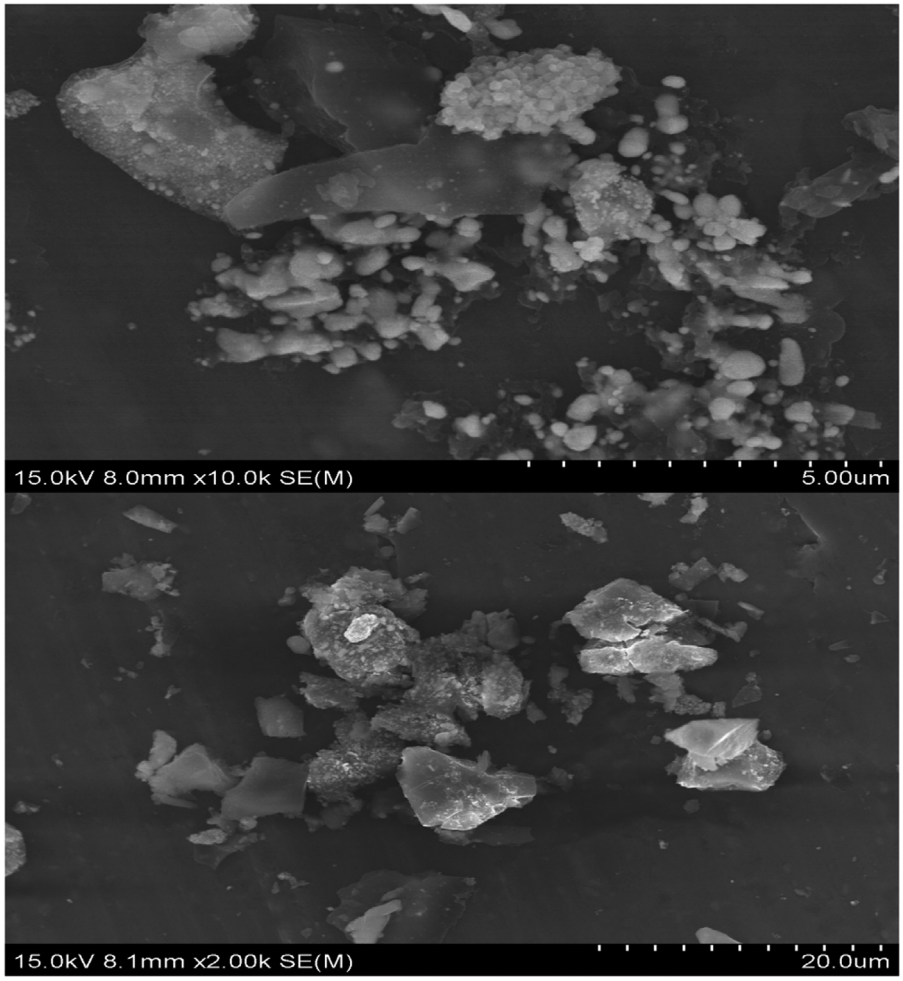

Fig. 11. FESEM images of adsorption of $C_{16}H_{18}ClN_3S$ for 50 gm.

observed decrease in adsorption capacity can be attributed to the saturation of adsorption sites during the process, whereas the number of available adsorption sites increases or to agglomeration or aggregation of adsorbent particles, which results in a reduction of the total adsorbent surface area and an increase in the diffusion path length .In a manner comparable to the adsorption of methylene Blue from water by a range of other adsorbent materials, including Salix babylonica leaves powder 2, citrus limetta peel 11, Phoenix tree's leaves 20, Lotus leaf 21, and orange peel powder 52, a similar effect of the adsorbent dose on the efficiency of methylene blue removal from water and on the adsorption capacity was observed [32,33].

Conclusion

The present investigation demonstrates a novel approach to the biosynthesis of AgNPs from orange and banana peel, which has been successfully applied to the treatment of textile wastewater. The synthesised AgNPs were observed to be spherical in shape with a diameter of approximately 38.02 nm, as seen in FESEM. The synthesised AgNPs demonstrated effective catalytic reduction activity after seven hours of treatment. Our study employed an expeditious method for the synthesis of stable silver nanoparticles (CPE-AgNPs), which were subsequently characterised using UV–vis spectroscopy, Fourier transform infrared spectroscopy (FTIR), and field-emission scanning electron microscopy (FESEM) analysis. Moreover, a substantial body of existing literature has focused its attention on surface-related analyses prior to degradation. The present study analyses the surface modulation subsequent to degradation. As a result, the findings may inform future research into the potential of various other nanoparticles for different synthetic dyes, both individually and as mixtures. This could contribute to the development of more effective treatment methods. Furthermore, it is crucial to assess the integration of the catalyst with conventional technologies, its stability, and its recyclability for long-term sustainability in real-world scenarios when considering industrial-scale technology. It can therefore be concluded that the photosynthesis of AgNPs using orange and banana peel extract is a cost-effective, simple and eco-friendly method that excludes the hazards arising from the use of harmful

reducing/capping agents. Furthermore, this process could be easily scaled up for industrial applications, thus significantly increasing the yield of the nanoparticles, which would undoubtedly establish its commercial viability in wastewater treatment.

Limitations

The sole limitation to this experiment is the quantity of the total yield. In order to obtain a satisfactory yield, it is necessary to process a considerable quantity of fruit peels

Ethics statements

None.

Declaration of competing interest

The authors declare that they have no known competing financial interests or personal relationships that could have appeared to influence the work reported in this paper.

CRediT authorship contribution statement

Jyolsna P: Conceptualization, Methodology, Formal analysis, Investigation, Writing – original draft, Writing – review & editing. **Gowthami V:** Investigation, Resources, Writing – review & editing, Supervision. **Hajeera Aseen A:** Resources.

Data availability

Data will be made available on request.

Acknowledgments

The authors thank all their colleagues for their unwavering support of this research.

References

[1] Y. Huo, S. Xiu, L. Meng, B. Quan, Solvothermal synthesis and applications of micro/nano carbons: a review, Chem. Eng. J. 451 (2023) 138572, doi:10.1016/j.cej.2022.138572.
[2] U. Manojkumar, D. Kaliannan, V. Srinivasan, B. Balasubramanian, H. Kamyab, Z.H. Mussa, J. Palaniyappan, M. Mesbah, S. Chelliapan, S. Palaninaicker, Green synthesis of zinc oxide nanoparticles using Brassica oleracea var. botrytis leaf extract: photocatalytic, antimicrobial and larvicidal activity, Chemosphere 323 (2023) 138263, doi:10.1016/j.chemosphere.2023.138263.
[3] I. Ijaz, A. Bukhari, E. Gilani, A. Nazir, H. Zain, R. Saeed, S. Hussain, T. Hussain, A. Bukhari, Y. Naseer, R. Aftab, Green synthesis of silver nanoparticles using different plants parts and biological organisms, characterization and antibacterial activity, Environ. Nanotechnol. Monit. Manage 18 (2022) 100704, doi:10.1016/j.enmm.2022.100704.
[4] M.T. Ishaq, A. Fazal, S. Ara, K. Sughra, One-pot greener synthesis of zinc oxide nanoflowers using potato, cauliflower, and pea peel extract with antibacterial application, Chem. Phys. Lett. 810 (2023) 140186, doi:10.1016/j.cplett.2022.140186.
[5] N. Sachin, N. Jaishree, N. Singh, R. Singh, K. Shah, B.K. Pramanik, Green synthesis of zinc oxide nanoparticles using lychee peel and its application in anti-bacterial properties and CR dye removal from wastewater, Chemosphere 327 (2023) 138497, doi:10.1016/j.chemosphere.2023.138497.
[6] K. Lee, M. Sahu, S. Hajra, R. Abolhassani, K. Mistewicz, B. Toroń, H. Rubahn, Y.K. Mishra, H.J. Kim, Zinc oxide tetrapod sponges for environmental pollutant monitoring and degradation, J. Mater. Res. Technol. J. Mater. Res. Technol. 22 (2023) 811–824, doi:10.1016/j.jmrt.2022.11.142.
[7] M. Ahmad, W. Rehman, M.M. Khan, M.T. Qureshi, A. Gul, S. Haq, R. Ullah, A. Rab, F. Menaa, Phytogenic fabrication of ZnO and gold decorated ZnO nanoparticles for photocatalytic degradation of Rhodamine B, J. Environ. Chem. Eng. 9 (1) (2021) 104725, doi:10.1016/j.jece.2020.104725.
[8] F.A. Alharthi, A.A. Alghamdi, N. Al-Zaqri, H.S. Alanazi, A.A. Alsyahi, A.E. Marghany, N. Ahmad, Facile one-pot green synthesis of Ag–ZnO Nanocomposites using potato peeland their Ag concentration dependent photocatalytic properties, Sci. Rep. 10 (1) (2020), doi:10.1038/s41598-020-77426-y.
[9] G. Ashrafi, M. Nasrollahzadeh, B. Jaleh, M. Sajjadi, H. Ghafuri, Biowaste- and nature-derived (nano)materials: biosynthesis, stability and environmental applications, Adv. Colloid. Interface Sci. 301 (2022) 102599, doi:10.1016/j.cis.2022.102599.
[10] N. Kaushal, A.K. Singh, Advancement in utilization of bio-based materials including cellulose, lignin, chitosan for bio-inspired surface coatings with special wetting behavior: a review on fabrication and applications, Int. J. Biol. Macromol. 246 (2023) 125709, doi:10.1016/j.ijbiomac.2023.125709.
[11] A. Verbič, K. Brenčič, M. Dolenec, G. Primc, N. Recek, M. Šala, M. Gorjanc, Designing UV-protective and hydrophilic or hydrophobic cotton fabrics through in-situ ZnO synthesis using biodegradable waste extracts, Appl. Surf. Sci. 599 (2022) 153931, doi:10.1016/j.apsusc.2022.153931.
[12] F. Sanakousar, C. Vidyasagar, V. Jiménez-Pérez, K. Prakash, Recent progress on visible-light-driven metal and non-metal doped ZnO nanostructures for photocatalytic degradation of organic pollutants, Mater. Sci. Semicond. Process. 140 (2022) 106390, doi:10.1016/j.mssp.2021.106390.
[13] K.S. Obayomi, A.E. Oluwadiya, S.Y. Lau, A.O. Dada, D. Akubuo-Casmir, T.A. Adelani-Akande, A.F. Bari, S.O. Temidayo, M.M. Rahman, Biosynthesis of Tithonia diversifolia leaf mediated Zinc Oxide Nanoparticles loaded with flamboyant pods (Delonix regia) for the treatment of Methylene Blue Wastewater, Arab. J. Chem. 14 (10) (2021) 103363, doi:10.1016/j.arabjc.2021.103363.
[14] R. Ishwarya, G. Tamilmani, R. Jayakumar, M.F. Albeshr, S. Mahboob, D. Shahid, M.N. Riaz, M. Govindarajan, B. Vaseeharan, Synthesis of zinc oxide nanoparticles using Vigna mungo seed husk extract: an enhanced antibacterial, anticancer activity and eco-friendly bio-toxicity assessment on algae and zooplankton, J. Drug Deliv. Sci. Technol. 79 (2023) 104002, doi:10.1016/j.jddst.2022.104002.
[15] B. Amudhavalli, R. Mariappan, M. Prasath, Synthesis chemical methods for deposition of ZnO, CdO and CdZnO thin films to facilitate further research, J. Alloys. Compd. 925 (2022) 166511, doi:10.1016/j.jallcom.2022.166511.
[16] K.B. Tan, D. Sun, J. Huang, T. Odoom-Wubah, Q. Li, State of arts on the bio-synthesis of noble metal nanoparticles and their biological application, Chin. J. Chem. Eng. Chin. J. Chem. Eng. 30 (2021) 272–290, doi:10.1016/j.cjche.2020.11.010.
[17] C. Pechyen, K. Ponsanti, B. Tangnorawich, N. Ngernyuang, Waste fruit peel – Mediated green synthesis of biocompatible gold nanoparticles, J. Mater. Res. Technol. J. Mater. Res. Technol. 14 (2021) 2982–2991, doi:10.1016/j.jmrt.2021.08.111.

[18] A.K. Singh, Engineered biochar for oil/water separation: processing and mechanism, Bioresour. Technol. Rep. 20 (2022) 101269, doi:10.1016/j.biteb.2022.101269.
[19] N.M.A. Niamke, N.S. Soro, N.B.T. Sea, N.J.E. Atchowo, N.J.A. Djaman, Characterization of the physicochemical properties of sweet pepper (Capsicum annuum) cultivated in Korhogo in the North of Côte d'Ivoire, GSC Adv. Res. Rev. 8 (3) (2021) 130–138, doi:10.30574/gscarr.2021.8.3.0204.
[20] A.K. Singh, A.K. Chaubey, I. Kaur, Remediation of water contaminated with antibiotics using biochar modified with layered double hydroxide: preparation and performance, J. Hazard. Mater. Adv. 10 (2023) 100286, doi:10.1016/j.hazadv.2023.100286.
[21] J.A. Kumar, T. Krithiga, S. Manigandan, S. Sathish, A.A. Renita, P. Prakash, B.N. Prasad, T.P. Kumar, M. Rajasimman, A. Hosseini-Bandegharaei, D. Prabu, S. Crispin, A focus to green synthesis of metal/metal based oxide nanoparticles: various mechanisms and applications towards ecological approach, J. Clean. Prod. 324 (2021) 129198, doi:10.1016/j.jclepro.2021.129198.
[22] Y. Jiang, P. Zhou, P. Zhang, M. Adeel, N. Shakoor, Y. Li, M. Li, M. Guo, W. Zhao, B. Lou, L. Wang, I. Lynch, Y. Rui, Green synthesis of metal-based nanoparticles for sustainable agriculture, Environ. Pollut. 309 (2022) 119755, doi:10.1016/j.envpol.2022.119755.
[23] S. Kumar, S.D. Lawaniya, S. Agarwal, Y. Yu, S.R. Nelamarri, M. Kumar, Y.K. Mishra, K. Awasthi, Optimization of Pt nanoparticles loading in ZnO for highly selective and stable hydrogen gas sensor at reduced working temperature, Sens. Actuat. B Chem. 375 (2023) 132943, doi:10.1016/j.snb.2022.132943.
[24] M. MuthuKathija, M.S.M. Badhusha, V. Rama, Green synthesis of zinc oxide nanoparticles using Pisonia Alba leaf extract and its antibacterial activity, Appl. Surf. Sci. Adv. 15 (2023) 100400, doi:10.1016/j.apsadv.2023.100400.
[25] S. Waseem, T. Sittar, Z.N. Kayani, S. Gillani, M. Rafique, M.A. Nawaz, S.M. Shaheen, M.A. Assiri, Plant mediated green synthesis of zinc oxide nanoparticles using Citrus jambhiri lushi leaves extract for photodegradation of methylene blue dye, Phys. B, Condens. Matter 663 (2023) 415005, doi:10.1016/j.physb.2023.415005.
[26] U. Manojkumar, D. Kaliannan, V. Srinivasan, B. Balasubramanian, H. Kamyab, Z.H. Mussa, J. Palaniyappan, M. Mesbah, S. Chelliapan, S. Palaninaicker, Green synthesis of zinc oxide nanoparticles using Brassica oleracea var. botrytis leaf extract: photocatalytic, antimicrobial and larvicidal activity, Chemosphere 323 (2023) 138263, doi:10.1016/j.chemosphere.2023.138263.
[27] T.U.D. Thi, T.T. Nguyen, Y.D. Thi, K.H.T. Thi, B.T. Phan, K.N. Pham, Green synthesis of ZnO nanoparticles using orange fruit peel extract for antibacterial activities, RSC. Adv. 10 (40) (2020) 23899–23907, doi:10.1039/d0ra04926c.
[28] R.H. Waghchaure, V.A. Adole, B.S. Jagdale, Photocatalytic degradation of methylene blue, rhodamine B, methyl orange and Eriochrome black T dyes by modified ZnO nanocatalysts: a concise review, Inorgan. Chem. Commun. Inorgan. Chem. Commun. (Online) 143 (2022) 109764, doi:10.1016/j.inoche.2022.109764.
[29] S. Chakraborty, J.J. Farida, R. Simon, S. Kasthuri, N. Mary, Averrhoe carrambola fruit extract assisted green synthesis of zno nanoparticles for the photodegradation of congo red dye, Surf. Interfaces. 19 (2020) 100488, doi:10.1016/j.surfin.2020.100488.
[30] P. Palai, S. Muduli, B. Priyadarshini, T.R. Sahoo, A facile green synthesis of ZnO nanoparticles and its adsorptive removal of Congo red dye from aqueous solution, Materials Today: Proceedings 38 (2021) 2445–2451, doi:10.1016/j.matpr.2020.07.387.
[31] P. Kulal, V. Badalamoole, Efficient removal of dyes and heavy metal ions from waste water using Gum ghatti – graft – poly(4-acryloylmorpholine) hydrogel incorporated with magnetite nanoparticles, J. Environ. Chem. Eng. 8 (5) (2020) 104207, doi:10.1016/j.jece.2020.104207.
[32] A. Podurets, V. Odegova, K. Cherkashina, A. Bulatov, N. Bobrysheva, M. Osmolowsky, M. Voznesenskiy, O. Osmolovskaya, The strategy for organic dye and antibiotic photocatalytic removal for water remediation in an example of Co-SnO2 nanoparticles, J. Hazard. Mater. 436 (2022) 129035, doi:10.1016/j.jhazmat.2022.129035.
[33] G. Kamarajan, D.B. Anburaj, V. Porkalai, A. Muthuvel, G. Nedunchezhian, Green synthesis of ZnO nanoparticles using Acalypha indica leaf extract and their photocatalyst degradation and antibacterial activity, J. Ind. Chem. Soc. 99 (10) (2022) 100695, doi:10.1016/j.jics.2022.100695.